Characterization of an In-house Built 50 Hz Single Dielectric Barrier Discharge System Having Asymmetric Electrodes

M. Y. Naz, A. Ghaffar, N. U. Rehman, S. A. Shahid and S. Shukrullah
1 Department of Mechanical Engineering, Universiti Teknologi PETRONAS, Bandar Seri Iskandar, 31750 Tronoh, Perak, Malaysia.
2, 4,5 Department of Physics, University of Agriculture, Faisalabad-Pakistan.
3 Department of Physics, COMSATS Institute of Information Technology, Islamabad-Pakistan.

***Abstract*— An in-house built asymmetric dielectric barrier discharge (DBD) system comprising of a 50 Hz high tension ac source and single dielectric barrier layer (quartz, glass) between two conducting electrodes is used to generate and sustain the micro-discharge plasmas of practical importance. Most of the DBDs of industrial interest are operated in this filamentary mode. The variations in transported charge and discharge power with increase in ac input voltage and barrier thickness are reported. Whereas, the optical emission spectroscopy technique with line intensity ratio method is used to determine the electron temperature and electron number density from recorded spectra as a function of ac input voltage, dielectric barrier thickness and inter-electrode air gap. It is observed that the applied voltage, type and thickness of dielectric barrier and inter-electrode air gap significantly influence the corresponding DBD plasma parameters.**

***Index Term*-- Atmospheric pressure plasmas, Step up transformer, Dielectric materials, Plasma processing**

I. INTRODUCTION

The chemical reactivity of non-local thermodynamical equilibrium discharge plasmas is of great importance in various material processing applications. The main advantage of these plasmas is the possibility of inducing sufficient surface chemical modifications at relatively higher working gas pressures. This feature of atmospheric pressure discharge plasmas necessitates the use of ambient air DBDs to answer to most of the surface engineering problems. Among the various tolls and techniques used for generation and sustainment of ambient air micro-discharge plasmas, the DBD technique is always favored because of its simple and flexible geometry [1, 2].

At atmospheric pressure, the DBDs usually consist of many micro-discharges having radius of the order of 100 µm. These discharges can be realized between two conductive electrodes separated by mean of an air gap and one solid dielectric barrier at least [1, 3]. These conducting electrodes are usually connected with high frequency power source for production of metastable species within discharge plasmas. These metastable species play a dominant role during the excitation of discharge plasmas through penning ionization. But the major drawbacks of high frequency DBD sources are the engineering cost, requirement of complicated impedance matching networks and excessive power losses via dielectric barrier heating. Under these circumstances, a low frequency (50 Hz) ac source consisting of a conventional step up transformer and a variac might be the best choice for generation of ambient air DBDs [4]. The low frequency DBD sources ranging from few Hz to few kHz require a simple or no impedance matching network. This feature makes these systems very cheaper and more practical in high pressure material processing applications.

The thermal, optical and electrical characterization of DBDs mainly dependents on the permittivity and thickness of the dielectric materials used [5, 6]. The ratio of relative permittivity to barrier thickness (ε_r / d) not only determines the power dissipated and amount of the charge transferred into gas discharge but also influences significantly the electron temperature, electron number density and density of the plasma reactive species [7]. Therefore, the electrical equivalent circuit [5] of an in-house built low frequency DBD system with mono-dielectric barrier between two conducting electrodes is shown in Fig. 1.

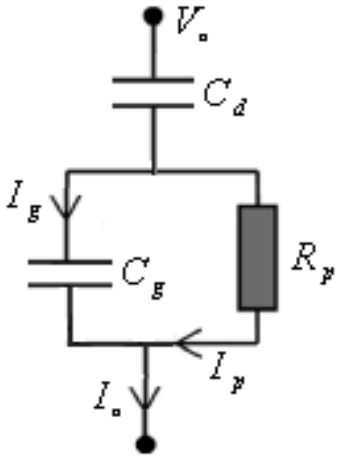

Fig. 1. Electrical equivalent circuit of the DBD system.

In this circuit, $V_\circ$ is the total applied voltage, $I_\circ$ is the corresponding current in circuit, C_g and C_d are the capacitance of inter-electrode air gap and dielectric barrier respectively. For effectiveness of the DBDs in plasma processing applications, some approximated formulae are used for evaluation of the optical and electrical characteristics of discharge plasmas. For example, the capacitance of the dielectric barriers can be determined using the equation [2]:

$$C_d = \frac{\varepsilon_r \varepsilon_\circ A}{d} \quad (1)$$

and the charge transferred into gas discharge per cycle of applied voltage across conducting electrodes can be determined as:

$$Q = 4\{C_d(V_P - V_b) - C_g V_b\} \quad (2)$$

Where, V_P and V_b is the applied voltage and breakdown voltage respectively.

Now the energy and power dissipated per cycle of applied voltage can be determined as follows:

$$E = QV_b = 4\{C_d(V_P - V_b) - C_g V_b\}V_b \quad (3)$$

$$P = \frac{E}{T} = fE \quad (4)$$

Whereas, the electron temperature and electron number density can be determined using optical emission spectroscopy (OES) technique. The spectroscopic characterization of the discharge plasmas is one of the most popular techniques know so far. It is a very reliable and simple in its implementation. It provides detailed information about plasma parameters such as the electron number density (n_e), electron temperature (kT_e), electron energy distribution function (EEDF), dissociation and ionization of discharge plasma species and densities of excited species [8, 9]. The details of OES measurements are discussed in next sections [6, 9].

So the present work includes the spectroscopic and to some extent the electrical characterization of ambient air DBD plasma with single dielectric barrier (quartz and glass) between two conducting electrodes. The atmospheric pressure DBD plasma is generated and sustained using a low frequency (50 Hz) source (comprises of a conventional step up transformer and a variac) at different excitation source voltages. The dielectric barrier capacitance, transported charge and energy and power dissipations are determined using equations (1)-(4), while the kT_e and n_e are a functioned from the spectroscopic data as function of excitation voltage, dielectric barrier thickness and inter electrode gap. The ultimate goal of the present work is to get control over discharge plasma parameters (such as charge transportation, energy and power dissipation, kT_e and n_e) for the optimization of low frequency DBD plasmas to be used in surface modification applications [10, 11].

II. MATERIALS AND METHODS

A. Asymmetric DBD Setup

The schematic diagram of an in-house built low frequency DBD system for generation and characterization of ambient air discharge plasmas is shown in Fig. 2.

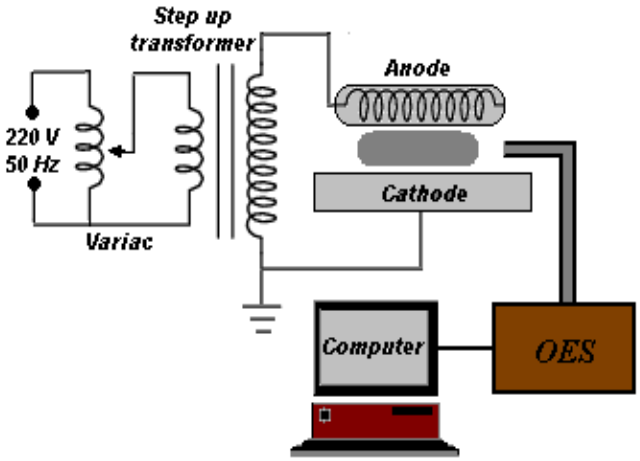

Fig. 2. Schematic diagram of asymmetric DBD system.

The asymmetric arrangement consists of an ac grounded aluminum electrode sheet (11 cm × 5 cm × 2 cm) and a spiral wound copper anode having 30 turns in total. The copper anode is mounted above the grounded aluminum sheet at an adjustable height of choice. Two kinds of dielectric barriers; quartz and glass with different thicknesses are used independently for DBD generation and characterization. Each dielectric barrier has its own specific relative permittivity thickness and capacitance as listed in Table I. The diameter of the copper anode is made of good fit inside the quartz and glass tubes [2, 12] (inner diameter 15 mm each).

The dielectric barrier covering of the spiral wound copper anode is the key for proper functioning of the atmospheric pressure DBDs. Without any dielectric barrier, the DBDs undergo to an arc transition region. However, the thickness of the dielectric barrier cover should be reasonably small to allow maximum ac power to pass through the dielectric barrier and cause electrical breakdown of the working gas. As in this experiment, only one electrode is covered with dielectric material, such type of DBDs can not be generated through dc sources. Therefore, a high tension ac

source comprising of a conventional step up transformer and a variac is used for generation of the atmospheric pressure DBD plasmas at 10, 11, 12, 13 and 14 kV. The step up transformer with 1:200 turn's ratio of primary to secondary winding may provide up to 50 kV with 200 mA current at the output terminals. For peak output value, the primary of the step up transformer consumes 250 V at 50 Hz frequency. The Variac is used to adjust the ac input of the step up transformer and to obtain the desired ac voltage at the output terminals. The digital multimeters are used for continuous monitoring of the voltages and currents across the DBD circuit.

The dielectric barrier capacitance, transported charge and energy and power dissipation are determined using the applied voltage and the data available in Table I. While, kT_e and n_e are evaluated from DBD induced spectroscopy.

TABLE I
Physical characteristics of tested dielectric barriers

Material	Barrier thickness (mm)	ε_r	ε_r/d $(1/mm)$	C_d (pF)
Quartz	1.0	4.22	4.220	3.74
	1.5		2.813	2.49
	1.8		2.344	2.08
Glass	1.0	8.63	8.630	7.64
	1.5		5.753	5.09
	1.8		4.794	4.25

The OES is carried out using a computer controlled system consisting of an Ocean Optic Spectrometer (HR: 4000 CG UV-NIR) and an optical fiber. The optical resolution of the spectrometer is 0.025 nm and the wavelength range of 200-1100 nm. With integration time of 4 ms to 20 s, the spectrometer can perform full scan into memory after every 4 ms with the USB 2.0 and after every 600 ms with the serial port. The light signal from the optical fiber is focused onto the slit via collimated lens, where it is collected by the detector of the spectrometer. The light sensitive semiconductor chip detector converts this optical signal into an electrical signal and transmits it to the computer, where the resultant spectra is recorded in the range of 300-600 nm as function of applied voltage, type and thickness of dielectric barrier and inter-electrode gap. The spectroscopic data is analyzed and influence of discharge plasma parameters on the spectral intensities of selected emission bands and lines is investigated.

B. Spectroscopic Characterization

In the present experiment, air is used as a working gas for the atmospheric pressure DBD generation. Having the atmospheric pressure and blend mixture of gases, it causes a series of chemical recombinations in the discharge which result into extinction of the discharge and therefore, large amount of energy (several keV) is required to generate and sustain the atmospheric pressure DBDs [2, 13]. When this energy reaches to a certain breakdown value, the glow discharge starts to grow with discrete filamentary distributions on dielectric barrier surface and becomes consistent with rise in applied voltage. In glow discharge plasmas, the electrons gain energy from the applied electric field and undergo inelastic collisions with neutral plasma species. Under such inelastic collisional processes, some of the neutral plasma species gain sufficient excitation energies and jump into higher energy states. Later on, these higher energy states decay back to lower energy states by emitting the photons of characteristic wavelengths. Using intensities of these spectral lines we can determine kT_e and n_e.

The OES technique used for determination of these parameters is based on measurement of relative intensities of two or four spectral lines of same atomic species [2, 12]. The intensity of these spectral lines depends on kT_e, and always proportional to the population density of excited states. Hence, kT_e can be determined using these spectral line intensities and well-know Boltzmann plot:

$$kT_e = \left(E_2 - E_1\right)\left[\ln\frac{I_1\lambda_1 g_2 A_2}{I_2\lambda_2 g_1 A_1}\right]^{-1} \quad (5)$$

The indices 1 and 2 refers to the first and second spectral lines, I is the intensity of the seleBoltzmannes, k is the Boltzman constant, g is the statistical weight, E is the excited state's energy and A is the transition probability. The Boltzmann plot method is only valid if the discharge plasma under study is in complete local thermodynamic equilibrium (LTE). But in the present case, it is difficult for this condition to hold due to low plasma densities and non-LTE character of DBD plasma [1, 2]. Therefore, this method may not be used for the exact determination of kT_e and n_e. Nevertheless, it can still provide us closely estimated values of these plasma parameters under different DBD working conditions [9]. A typical DBD spectrum with quartz dielectric barrier and 1 mm inter-electrode gap at 10 kV ac input is shown in Fig. 3a.

In this spectrum, the nitrogen and oxygen emitted lines are observed in the range of 300-600 nm and kT_e is determined by selecting two N-I spectral lines. These spectral lines result from the transition of $^3P_{3/2}$ state to $^3S_{1/2}$ state at 409.99 nm and $^5P_{3/2}$ state to $^3S_{3/2}$ state at 390.01 nm. The intensity of these spectral lines is obtained from the observed spectrum by integrating over line profile and normalizing with the spectral response of the instrument. The E, g and A for selected lines is taken from the NIST Atomic Spectra Datasheet. Using all these values in equation (5), the kT_e can easily be determined as function of applied voltage, inter-

electrode air gap and barrier thickness as shown in Fig. 6. Whereas, the n_e can be determined using the relative intensities of atomic and ionic spectral lines in Boltzman-Saha equation.

$$n_e = [(2\pi mkT_e)^{3/2}/h^3][2A^+g^+\lambda^0 I^0/A^0g^0\lambda^+I^+]\times \exp[-(E^+ - E^0 + E_i{}^0 - \Delta E_i)/kT_e] \quad (6)$$

Where, (0, +) denote the neutral and ionized atoms, E is the energy of the emissive levels, $E_i{}^0$ is the ionization energy of the neutral atoms and ΔE_i is the lowering of ionization energy. The N-I and N-II lines used for the determination of n_e are identified and labeled in Fig. 3b. These lines result from the atomic transition of $^5P_{3/2}$ state to $^3S_{3/2}$ state at 390.01 nm and ionic transition of $4S$ state to $3P$ state at 366.38 nm.

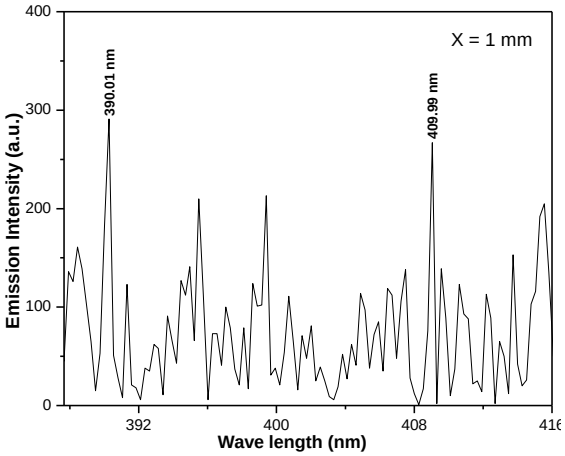

Fig. 3a. The emission spectrum recorded at 10 kV for determination of kT_e.

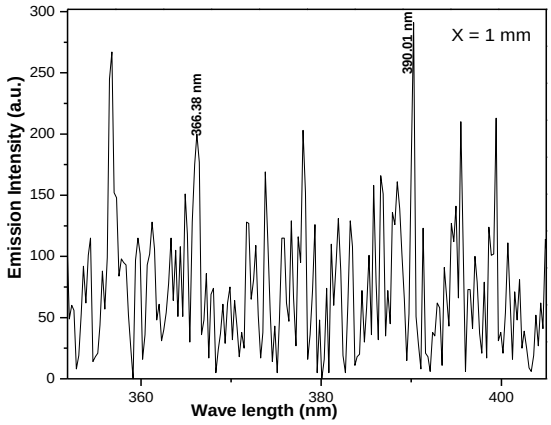

Fig. 3b. The emission spectrum recorded at 10 kV for determination of n_e.

III. RESULTS AND DISCUSSION

A. DBD Reaction Kinetics

The use of OES technique for the determination of average electron energy in discharge plasmas requires careful analysis of the kinetic processes involved in population and depopulation of excited states of the discharge plasma species. In ambient air DBDs, the highly energetic electrons play a very important role during excitation and ionization of the corresponding oxygen and nitrogen species. Some of the most important chemical reactions induced by these energetic electrons are as follows [1, 2]:

$$O_2 + e \longrightarrow O + O + e$$

and three body reaction generates the ozone as:

$$O + O_2 + M \longrightarrow O_3 + M$$

For nitrogen:

$$e + N_2(X^1\Sigma_g^+)\upsilon = 0 \longrightarrow N_2(C^3\Pi_u)\upsilon' = 0 + e$$

Where, $N_2(C^3\Pi_u)$ state can be populated by many excitation and quenching processes like: penning excitation, associative excitation, electron impact excitation (from ground state $N_2(X^1\Sigma_g^+)$ and first metastable state $N_2(A^3\Sigma_u^+)$), pooling reactions and energy transfer between colliding particles [9]. The radiative decay of the subsequent states results into the characteristic photons of (0-0) band of second positive system at 337.1 nm which are identified in the recorded spectrum [12].

The second positive system of nitrogen (N_2^*) can also lead to the formation of oxygen atoms by the following reactions:

$$N_2 + e \rightarrow N_2^* + e$$

$$N_2^* + O_2 \rightarrow N_2 + 2O$$

$$N_2^* + O_2 \rightarrow N_2O + O$$

$$O + O_2 + M \rightarrow O_3 + M$$

Similarly, the direct impact ionization from the ground state $N_2(X^1\Sigma_g^+)$ populates the $N_2^+(B^2\Sigma_u^+)$ excited state [12].

$$e + N_2(X^1\sum_g^+) \rightarrow N_2^+(B^2\sum_u^+) + 2e$$

Again, the $N_2^+(B^2\sum_u^+)$ excited state emits the characteristic photons of (0-0) band of first negative system as identified in recorded spectrum [9, 12]. The emission intensity of the band is proportional to the population density of the $N_2^+(B^2\sum_u^+)\upsilon' = 0$ state.

$$N_2^+(B^2\sum_u^+)\upsilon' = 0 \rightarrow N_2^+(X^2\sum_g^+)\upsilon = o + h\upsilon$$

In atmospheric pressure DBDs, the dissociation of nitrogen molecules due to the direct impact of the electrons is also an important discharge plasma parameter which plays a very crucial role in DBD processing applications. The following chemical kinetics are involved in the nitrogen dissociation [1, 2, 16].

$$e + N_2(X^1\sum_g^+, \nu = 0) \rightarrow e + N(^4S) + N(^4S)$$

$$e + N_2(X^1\sum_g^+, \nu = 0) \rightarrow e + N(^4S) + N(^2D)$$

So the dissociation of nitrogen and oxygen molecules results in the production of N and O radicals. At atmospheric pressure these radicals have very high concentrations and chemical reactivates which is desirable in DBD processing applications. Particularly, the pulsed mode atmospheric pressure DBDs as presented in this paper can also sterilize against almost all the types of bacteria due to very high concentrations of ionic and reactive species [13-15].

B. DBD Plasma Parameters

The variational trend of both discharge power and transported charge with a rise in applied voltage and dielectric barrier thickness is shown in Fig. 4 & 5. The inter electrode gap was kept constant at 1mm and corresponding response of discharge power and transported charge is observed. For all cases in Fig. 4a & 4b, it can be noted that both plasma parameters have proportional relation with rising ac input voltage which is in good agreement with the results reported by Kim and Abdel-Salam [15, 16]. Where in Fig. 5a & 5b, there is an inverse but non-linear relationship between the discharge plasma parameters and dielectric barrier thickness. It means, thicker the dielectric barrier is, lower will be the discharge power and transported charge. Furthermore, it is found that discharge power and transported charge for glass as dielectric barrier are higher than those for quartz due to higher relative permittivity and capacitance as shown in Table I.

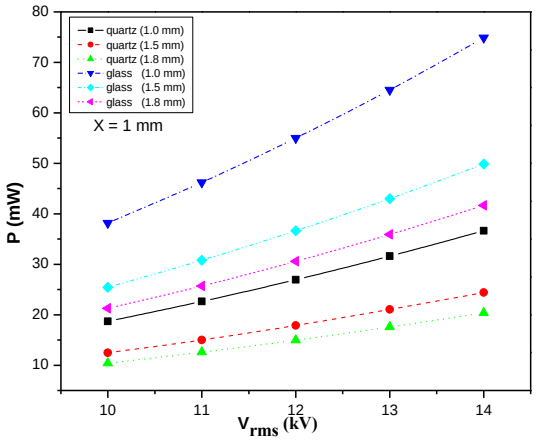

Fig. 4a. Variational trend of discharge power with applied voltage.

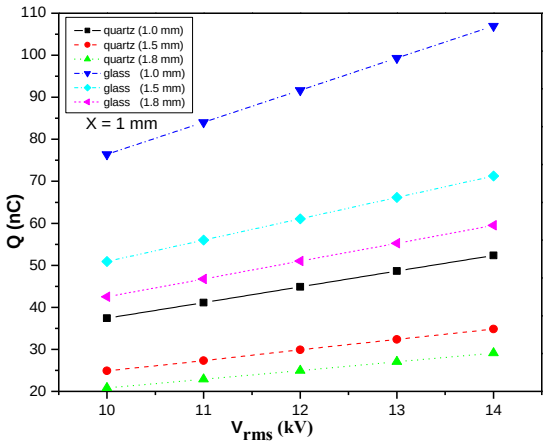

Fig. 4b. Variational trend of transported charge with applied voltage.

The equations (1)-(4) show that the discharge plasma parameters depend only on applied voltage, dielectric thickness, inter-electrode gap and relative permittivity because all other parameters are kept constant. The discharge power and transported charge become proportional to the applied voltage when relative permittivity, inter-electrode gap and dielectric barrier thickness are fixed. Under this condition the breakdown voltage remains constant while the difference of applied voltage and breakdown voltage in discharge gap increases with rise in applied voltage. More and more discharge power will be consumed and consequently higher charge transportation with applied voltage takes place. Now, by fixing the applied voltage, relative permittivity and inter-electrode gap, the discharge power and charge transportation can only be regarded as a function of dielectric barrier thickness. From equations (1)-(4), it can be seen that both discharge power and transported charge decrease with increase in dielectric barrier thickness due to reduction in mean current density, the discharge glow becomes weak under these conditions [17].

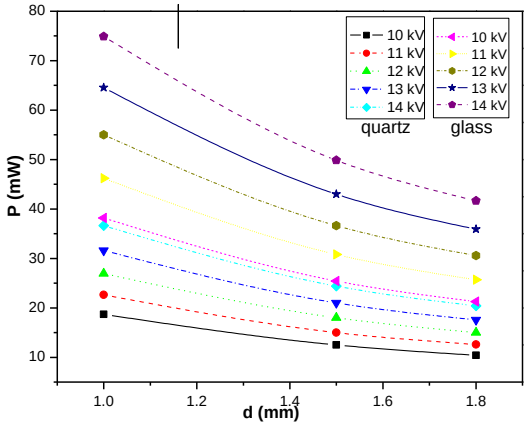

Fig. 5a. Variational trend of discharge power with dielectric barrier thickness.

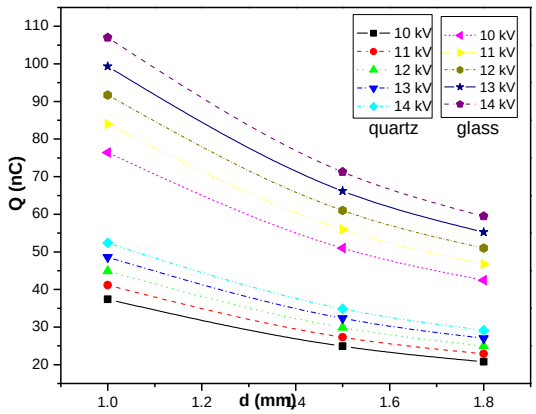

Fig. 5b. Variational trend of transported charge with dielectric barrier thickness.

The spectroscopic results for kT_e and n_e as function of applied voltage and barrier thickness (1, 1.5, 1.8 mm) are shown in Fig. 6 & 7. In discharge plasmas, the kT_e not only controls the production rate of active species via inelastic collisions but also helps in determination of rate processes of discharge plasma reactive gases. Therefore, kT_e values should always be regulated to get good control over selected processes occurring in DBDs. In Fig. 6, it can easily be noted that kT_e increases with rise in applied voltage [18]. This increasing trend in kT_e might be due to the rise in kinetic energy of the electrons in DBD. But the most promising argument is the availability of more energetic electrons in high energy tail of the electron energy distribution function at relatively higher values of applied voltage [19]. As the relation for mean energy of electrons is [2]:

$$\bar{E} = qE_e\lambda_e = \frac{qV\lambda_e}{X} = \frac{q\pi r_i^2}{Xk_BT}\left(\frac{V_{rms}}{P}\right) \quad (7)$$

In this equation, E_e is the electric field strength, λ_e is the mean free path V is the applied voltage, X is the inter-electrode gap, r_i is the ionic radius and k_B is the Boltzmann constant. From the equation (7), it is clear that at constant atmospheric pressure, the electron mean free path in discharge plasma remains constant, but with rise in applied voltage, the availability of highly energetic electrons capable of ionizing the neutral species also increases and consequently the kT_e values. This incremental trend in excitation and ionization processes with applied voltage also has direct impact on n_e. Furthermore, the low frequency DBDs are composed of many micro-discharges. These micro-discharges increase in number with the rise in applied voltage which indirectly a prediction of an increase in n_e. It can also seen in equation (6) that there is a direct relation between n_e and kT_e. It means, if kT_e increases, the n_e will automatically increase as observed in this investigation.

Not only the applied voltage but the type and thickness of dielectric barrier material used also have significant effects on atmospheric pressure DBD parameters as demonstrated in Fig. 6 & 7. The results are obtained with quartz and glass dielectric barriers of same thickness of 1, 1.5 and 1.8 mm. It can be anticipated that the increasing barrier thickness has adverse effects on both kT_e and n_e. It means, thicker the dielectric barrier, lower will be the ε_r/d ratio and fewer charge transportation will take place. Hence, even at constant applied voltages, the electron temperature and density of the excited states decrease with increase in dielectric barrier thickness. So in above discussion, it can be concluded that the thinner dielectric barriers with higher relative permitivities are desirable for the enhancement of electron temperature and densities of the DBD reactive species for material processing applications. However, thinner dielectric barriers may also have some adverse effects on the DBD parameters. For example, if thickness of the dielectric barrier is too short, there is a possibility of going the electrical breakdown into an arc region [5]. In order to overcome this problem, the use of the dielectric barriers with higher relative permitivities is recommended rather than thinner dielectric barriers. Higher relative permitivities permit high values of the charge to be transported without occurrence of any breakdown. The results in Fig. 6 & 7 also confirm that the kT_e and n_e values for glass ($\varepsilon_r = 8.63$) are much higher than those obtained with quartz ($\varepsilon_r = 4.22$) of same barrier thickness. It is a confirmation of fact that the efficiency of the DBD systems

can be enhanced by using the dielectric materials of higher ε_r values [5].

Another problem faced while using the thinner dielectric barriers is that the n_e and kT_e become independent of system parameters and physical properties of the dielectric material in particular. In Fig. 8, it is predicted that although, the relative permittivity of the glass is much higher than quartz but the DBD parameters determined using quartz and glass are comparable for barrier thickness of 1 mm. For thinner dielectric barriers, the observed behavior might be due to the higher secondary electron emission coefficient (SEEC) of the quartz dielectric. The SEEC plays a dominant role in DBDs generated with thin dielectric barriers.

Finally, the inter-electrode air gap effects on atmospheric pressure DBD parameters are also investigated as shown in Fig. 9. It can be seen that both kT_e and n_e decrease with increase in inter-electrode air gap. From the equations (1)-(4), the variational trend of the investigated DBD plasma parameters with inter-electrode air gap can easily be justified [5, 9, 12, 15].

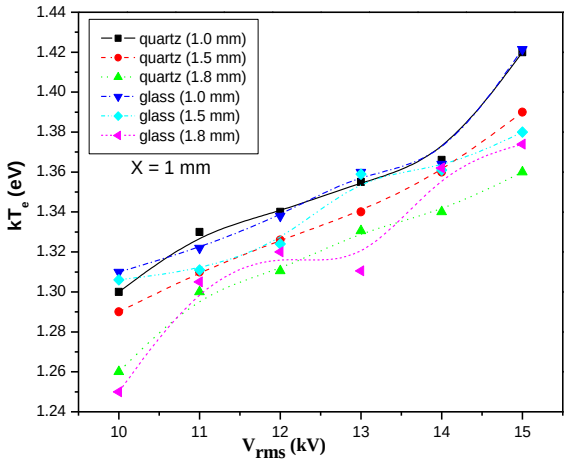

Fig. 6. Variational trend of electron temperature with applied voltage.

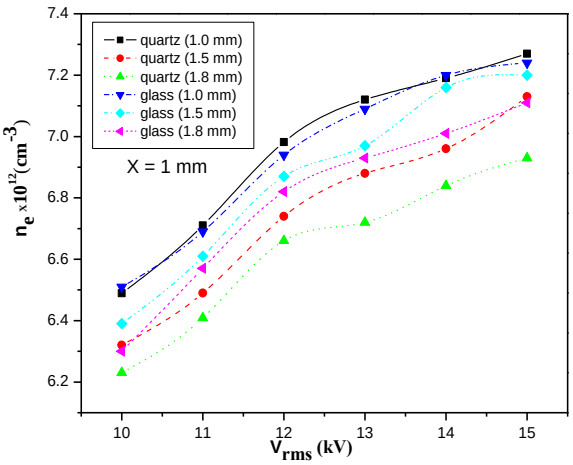

Fig. 7. Variational trend of electron number density with applied voltage.

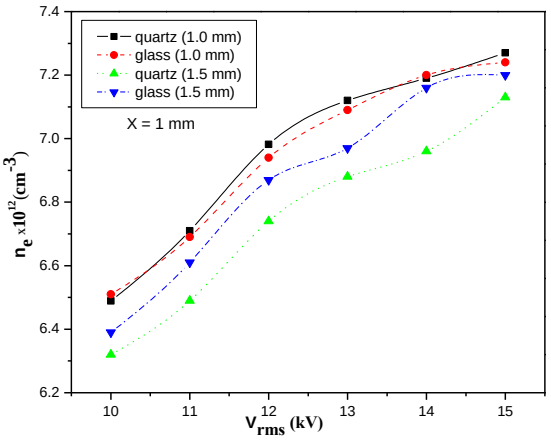

Fig. 8a. Comparison of electron number density for quartz & glass dielectric barriers.

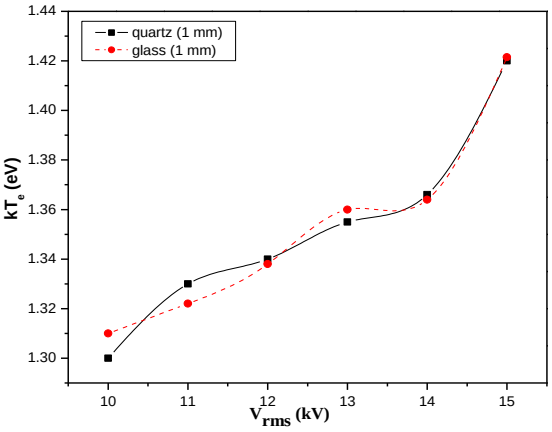

Fig. 8b. Comparison of electron temperature for quartz & glass dielectric barriers.

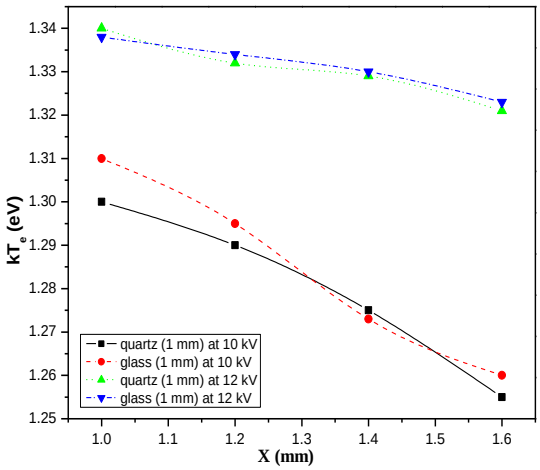

Fig. 9a. Variational trend of electron temperature with inter-electrode air gap.

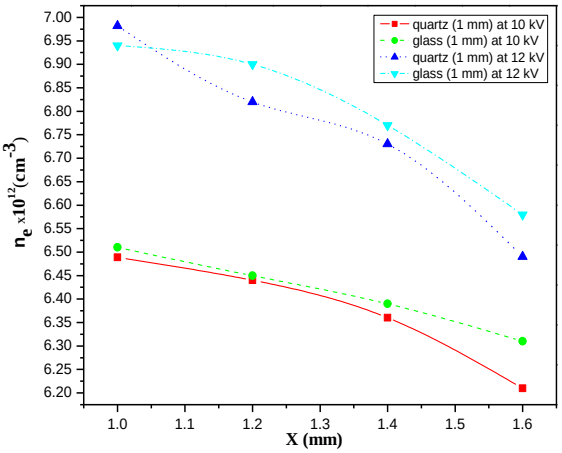

Fig. 9b. Electron number density versus inter-electrode gap.

IV. CONCLUSIONS

An in-house built ambient air DBD system with single dielectric barrier layer between asymmetric conducting electrodes is excited by high tension ac source comprising of a 50 Hz step up transformer and a variac. The quartz and glass dielectric barriers having a range of layer thicknesses are used for DBD generation independently. The spectroscopic and to some extent electrical characterization of atmospheric pressure DBD plasma is carried out, discharge power, transported charge, electron temperature and number density are determined as function of applied voltage, dielectric barrier thickness, inter-electrode air gap and relative permittivity of dielectric material. It is observed that the physical properties of the dielectric barrier appreciably influence the DBD plasma parameters. It is also observed that all DBD parameters increase with rise in applied voltage and show an inverse trend with an increase in dielectric barrier thickness and inter-electrode air gap. Finally, it is concluded that the glow discharge reactivity can be enhanced by use of thinner dielectric barriers, but for very thin barrier layers, the DBD can go into an arc region. Very thin dielectric barriers can only be useful when they have high secondary electron emission coefficients. So it will be safe and advantageous to use the dielectric materials with higher relative permitivities rather than very small thickness.

IV. REFERENCES

[1] F. Massines, P. Segur, N. Gherardi, C. Khanphan, A. Ricard, *Surf. Coat. Technol.* **174,** 8 (2003)

[2] M. Y. Naz, A. Ghaffar, N. U. Rehman , S. Shukrullah, M. A. Ali, *PIER M* **24,** 193 (2012)

[3] K. Kale, S. Palaskar, P. J. Hauser, A. El-Shafei, *Indian J. Fibre Text. Res.* **36,** 137 (2011)

[4] N. Osawa, Y. Yoshioka, *IEEE Trans. Plasma Sci.* **40,** (2011)

[5] A. Meiners, M. Leck, B. Adel, *Rev. Sci. Instrum.* **81,** 113507 (2010)

[6] S. D. Anghel, *IEEE Trans. Plasma Sci.* **39,** (2011)

[7] U. Kogelschatz, *Plasma Phys. Contr. F.* **46,** (2004)

[8] R. S. Yadav, A. F. Khan, H. Chander, D. Haranath, A. Yadav, A. K. Sharma, S, Chawla, *Indian J. Pure Appl. Phys.* 47, 399 (2009)

[9] F. U. Khan, N. U. Rehman, S. Naseer, M. A. Naveed, A. Qayyum, N. A. D. Khattak, M. Zakaullah, *Eur. Phys. J. Appl. Phys.* **45,** 11002 (2009)

[10] B. Ganguli, *Indian J. Pure Appl. Phys.* **49,** 759 (2011)

[11] D. P. Subedi, D. K. Madhup, K. Adhikari, U. M. Joshi, *Indian J. Pure Appl. Phys.* **46,** 540 (2008)

[12] G. Borcia, N. M. D. Brown, D. Dixon, R. McIlhagger, *Surf. Coat. Technol.* **179,** 70 (2004)

[13] R. Castell, E. J. Iglesias, and J. Ruiz-Camacho, *Braz. J. Phys.* **34** (4B), 1734 (2004)

[14] B.N. Sismanoglu, C.L.A. Cunha, M.P. Gomes, R. Caetano, K.G. Grigorov, *Braz. J. Phys.* **40** (4), 459 (2010)

[15] Y. Kim, K. T. Kim, M. S. Cha, Y. H. Song, S. J. Kim, *IEEE Trans. Plasma Sci.* **33,** 1041 (2005)

[16] M. Abdel-Salam, H. Sigger, A. Ahmed, *J. Phys. D: Appl. Phys.* **34,** 1219 (2001)

[17] C. Chen, Wen-Ya Chang, *Indian Journal of Fibre & Textile Research* 32, 122 (2007)

[18] M. Y. Naz, A. Ghaffar, N. U. Rehman, M. Azam, S. Shukrullah, A. Qayyum, M. Zakaullah, *PIER* **115,** 207 (2011)

[19] M. Y. Naz, A. Ghaffar, N. U. Rehman, S. Naseer, M. Zakaullah, *PIER* **114,** 113 (2011)